

Raman activity of sp^3 carbon allotropes under pressure: A density functional theory study

José A. Flores-Livas,¹ Lauri Lehtovaara,¹ Maximilian Amsler,² Stefan Goedecker,² Stéphane Pailhès,¹ Silvana Botti,^{1,3} Alfonso San Miguel,¹ and Miguel A. L. Marques¹

¹Université de Lyon, F-69000 Lyon, France and Laboratoire de Physique de la Matière Condensée et Nanostructures, Centre National de la Recherche Scientifique, UMR 5586, Université Lyon 1, F-69622 Villeurbanne, France

²Department of Physics, Universität Basel, Klingelbergstr. 82, 4056 Basel, Switzerland

³Laboratoire des Solides Irradiés (LSI) and ETSF, École Polytechnique, CNRS, CEA-DSM, F-91128 Palaiseau, France
(Received 11 November 2011; revised manuscript received 14 February 2012; published 13 April 2012)

Raman spectroscopy is a powerful tool to study the intrinsic vibrational characteristics of crystals, and, therefore, it is an adequate technique to explore phase transitions of carbon under pressure. However, the diamond-anvil cell, which is used in experiments to apply pressure, appears as a broad intense feature in the spectra. This feature lies, unfortunately, in the same range as the principal modes of recently proposed sp^3 carbon structures. As these modes are hard to distinguish from the diamond cell background, we analyze all Raman-active modes present in the sp^3 carbon structures in order to find detectable fingerprint features for an experimental identification.

DOI: 10.1103/PhysRevB.85.155428

PACS number(s): 81.05.uf, 81.40.Vw, 78.30.Fs, 63.22.Kn

The phase transition in compressed graphite has been thoroughly studied since pioneering works in the 1960s.^{1–5} Experimental evidence suggests that graphite undergoes a phase transition to a superhard phase in the range of 10 to 20 GPa.^{6,7} From the theoretical side, the pressure-induced phase transition of graphite has also been intensively studied.⁸ In particular, sophisticated *ab initio* crystal structure prediction methods, such as evolutionary algorithms,^{9–11} random sampling,^{12,13} particle-swarm optimization,¹⁴ and the minima hopping method,^{15,16} have also been employed to discover several possible crystal structures of carbon. These include three-dimensional arrangements of carbon nanotubes,¹⁷ superdense and superhard carbon allotropes,^{18–20} hybrid sp^2 - sp^3 diamond-graphite structures,^{21,22} *M*-carbon,²³ *BcT* carbon,^{24,25} *W*-carbon,²⁶ and *Z*-carbon,^{27–29} to name a few. As most of the proposed sp^3 structures become more stable than graphite in the range of 10–20 GPa, any of them could explain the experimental observations. A few attempts have been made to clarify this situation, in which the focus has been on the electronic structure and on optical and mechanical properties.³⁰ However, none of the results is fully convincing, and the structure behind the observed phase transition remains ambiguous.

One of the most significant features of Raman spectroscopy is that it provides a unique fingerprint of the intrinsic vibrational properties of a crystal. Therefore, Raman spectroscopy is an adequate technique to explore the phase transitions of compressed graphite. However, complications arise from the diamond-anvil cells commonly used in high-pressure experiments: the T_{2g} optical mode of cubic diamond leads to an intense and broad feature at 1332.5 cm^{-1} (at ambient conditions), and this extends to higher frequencies as pressure is increased. Unfortunately, this feature lies in the same spectral range of the principal Raman-active modes of the recently proposed sp^3 carbon structures. Therefore, just by looking at frequencies around the diamond peak, it is very hard to distinguish a possible signal coming from the sample from the background signal of the cell.

In addition to the principal vibrational modes, all proposed phases have several other Raman-active modes. As these

structures belong to different crystal families (e.g. monoclinic or orthorhombic), lattice vibrations are different and therefore can exhibit different Raman activity. Moreover, the evolution of the modes with respect to increasing pressure provides additional information to compare with experiments. In this article, we present all first-order Raman-active modes and their pressure dependence for recently proposed sp^3 carbon allotropes. We furthermore present nonresonant Raman spectra calculated at high pressure. Our results provide fingerprints for an experimental confirmation of the structural transformation in compressed graphite.

The ensemble of carbon structures studied in this work is shown in Fig. 1. We include, as reference systems, cubic diamond ($Fd-3m$) and hexagonal diamond ($P6_3/mmc$). Furthermore, we study the recently proposed sp^3 carbon allotropes: (i) *M*-carbon,²³ a monoclinic system ($C2/m$) with 8 atoms per primitive cell; (ii) *BcT* carbon,^{24,25} a tetragonal system ($I4/m$) with 4 atoms per cell; (iii) *W*-carbon,²⁶ an orthorhombic system ($Pnma$) with 16 atoms per cell; and (iv) *Z*-carbon,²⁷ an orthorhombic system ($Cmmm$) with 8 atoms per primitive cell.

Our calculations were performed using density-functional theory with the ABINIT package.³¹ We used Troullier-Martins pseudopotentials³² and the local-density approximation (LDA) to the exchange-correlation functional. The choice of the LDA is related to the fact that this functional performs well for both sp^2 and sp^3 carbon. Results obtained with the Perdew-Burke-Ernzerhof exchange-correlation functional³³ can be found in the Supplemental Material.³⁴ The plane-wave cutoff energy for all runs was 30 hartree, and k -point meshes were constructed with the Monkhorst-Pack scheme: $8 \times 8 \times 8$ for 16-atom cells, $12 \times 12 \times 12$ for 8-atom cells, and $16 \times 16 \times 16$ for 4-atom cells. Phonon and Raman calculations were performed within density-functional perturbation theory as implemented in ABINIT.^{35–37} The Raman activity of the crystals was determined by group-theoretical selection rules based on the space group, the mode symmetry, and the atomic sites. The nonresonant Raman intensities were averaged isotropically to obtain the powder spectra,³⁸ which was broadened by a Lorentzian with half width at half maximum of 10 cm^{-1} .

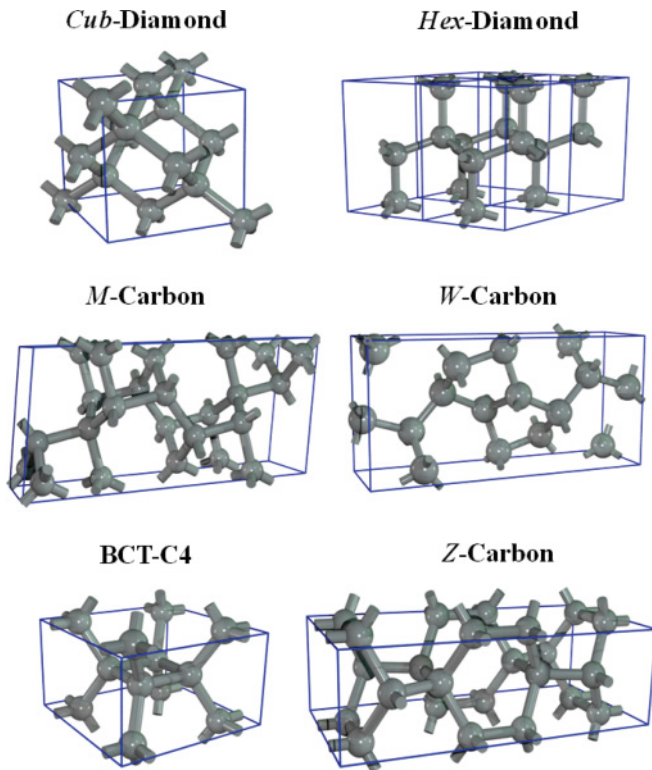


FIG. 1. (Color online) Carbon structures with the sp^3 tetrahedral bond studied in this work: cubic diamond, hexagonal diamond, M -carbon (monoclinic), BcT carbon, W -carbon (orthorhombic), and Z -carbon (orthorhombic).

Our main results are summarized in Fig. 2, where we present the zone-center, Raman-active phonons of the selected structures as a function of pressure. Shaded (green) areas in the panels mark the experimental evolution of the diamond-anvil cell background up to the pressure of 35 GPa.^{39,44} We remark that the diamond signal and its pressure evolution have been extensively studied both experimentally and theoretically.^{39–45} The Raman-active modes, their pressure coefficients, and Grüneisen parameters are also given in the Supplemental Material.³⁴ In panel (a) of Fig. 2, the solid black line represents the calculated optical mode of cubic diamond, T_{2g} . The dashed blue lines are modes characteristic of hexagonal diamond, whose mechanical representation is $\Gamma^{\text{Hex}} = A_{1g} + E_{1g} + E_{2g}$. Note that our calculations are in good agreement with previously reported values.^{45–47} For BcT carbon the Raman-active modes are $\Gamma^{BcT} = A_{1g} + B_{1g} + B_{2g} + E_g$ and are also shown in panel (a). The A_{1g} mode is a longitudinal optical mode vibrating at 1350 cm^{-1} at 0 GPa, a frequency higher than the T_{2g} mode of cubic diamond and with a larger variation with applied pressure. Other features present in BcT carbon are the B_{1g} mode and the E_g mode, the latter stemming from the doubly degenerate in-plane vibration of the four-member carbon rings (squares) present in the structure. These modes are below the diamond area and should appear as a small shoulder in Raman measurements above a pressure of 18.4 GPa—the pressure at which this structure becomes more stable than graphite.²⁴

Panel (b) of Fig. 2 shows the Raman modes of M -carbon, $\Gamma^M = A_g + B_g$. Two modes can be used to fingerprint the

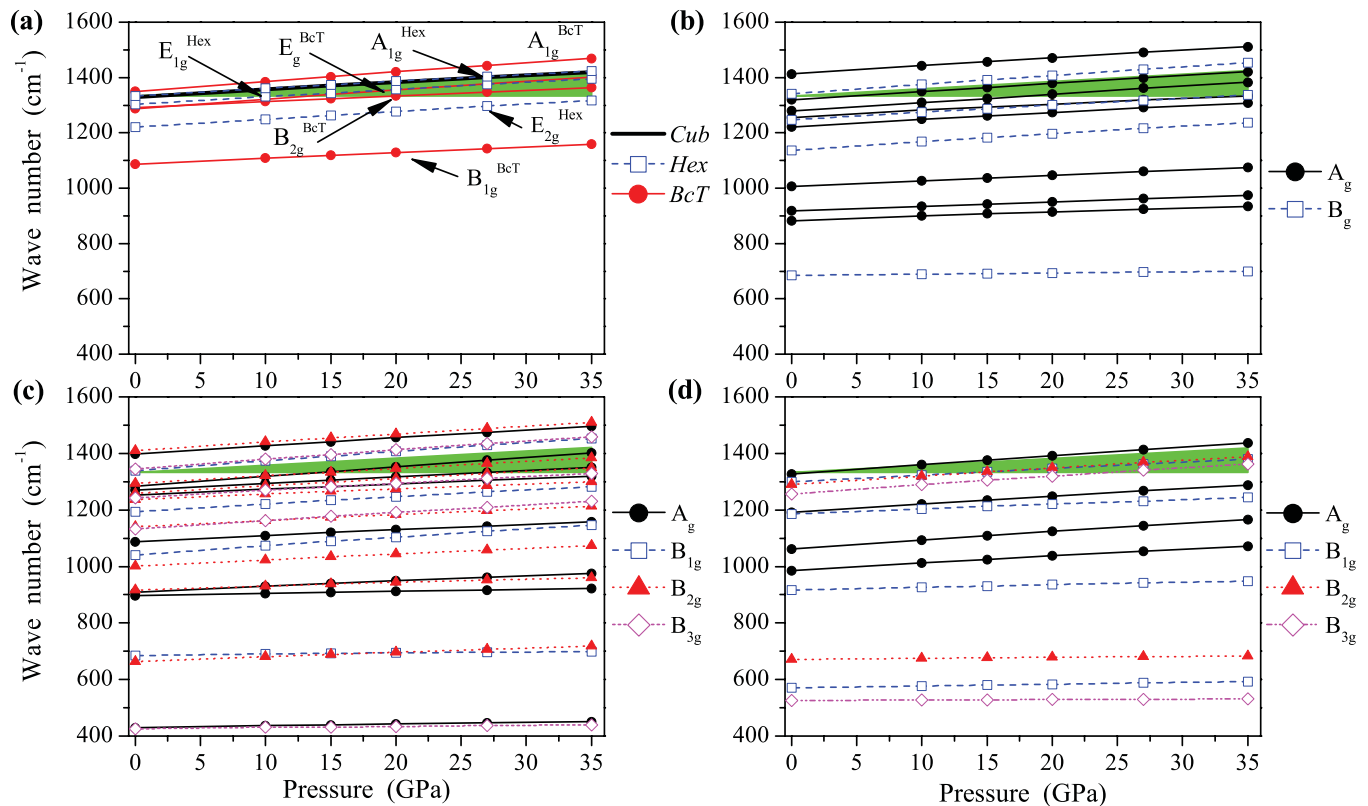


FIG. 2. (Color online) Calculated Raman-active modes of the sp^3 carbon structures studied in this work as a function of pressure: (a) cubic diamond, hexagonal diamond, and BcT carbon; (b) M -carbon (monoclinic); (c) W -carbon (orthorhombic); and (d) Z -carbon (orthorhombic).

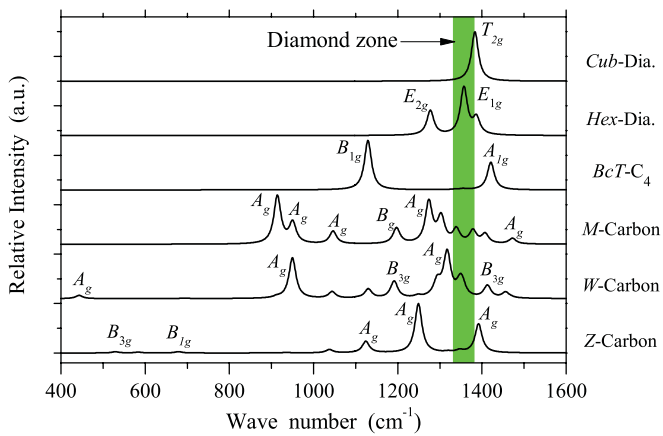


FIG. 3. (Color online) Raman spectra calculated for sp^3 carbon allotropes at 20 GPa. The green area represents the experimental evolution of the diamond peak under pressure. Only principal modes are labeled.

structure: The highest A_g mode is an in-phase mode which appears above the diamond zone with a pressure dependence similar to the T_{2g} mode of cubic diamond; the B_g mode at 680 cm^{-1} is an antiphase vibration which has sublinear pressure dependence; i.e., it is a tough mode.

The Raman modes of W -carbon are $\Gamma^W = 2A_g + B_{1g} + 2B_{2g} + B_{3g}$, and for Z -carbon $\Gamma^Z = 4A_g + 4B_{1g} + 2B_{2g} + 2B_{3g}$ [see panels (c) and (d), respectively]. Note that these two crystals belong to the same point group. The A_g mode is the usual in-phase mode and the B_g is a nondegenerate antiphase mode (the number in subscript refers to how the mode transforms with respect to the different mirror planes). A significant feature in W - and Z -carbon is that these two structures possess Raman-active modes at frequencies lower than the rest of the sp^3 structures. The lowest vibrations and Raman-active modes of W -carbon are the A_g and the B_{3g} modes at around 427 cm^{-1} , and the lowest modes on Z -carbon are the B_{3g} and the B_{1g} modes at around 525 and 570 cm^{-1} , respectively. These modes have a sublinear pressure dependence and could be distinguishable in experiments. However, the B -type modes are active only along certain directions of crystal symmetry and polarization conditions. Therefore, they are harder to explore experimentally.

In Fig. 3 we show the first-order Raman spectra calculated for different sp^3 carbon structures at 20 GPa. BcT carbon presents two modes with relatively large intensities which lie outside the diamond zone: the A_{1g} at 1420 cm^{-1} and the B_{1g} at 1127 cm^{-1} . For M -carbon the modes with larger scattering efficiency are those with A_g symmetry at 913 , 1273 , and 1472 cm^{-1} . For W -carbon the mode with the highest scattering efficiency is just above the diamond zone at 20 GPa. This phonon has A_g symmetry and a frequency of 1320 cm^{-1} .

Finally, Z -carbon exhibits three large peaks at 1125 , 1390 (above the diamond zone), and 1250 cm^{-1} (the principal mode).

Finally, we would like to discuss the possibility of the existence of these sp^3 structures in μ -Raman-scattering experiments of meteorites.⁴⁸ The samples are essentially constituted by hexagonal-like structures (lonsdaleites) of carbon; however, several “uncategorized” peaks are present in their spectra. These spectra exhibit a peak at around 430 cm^{-1} (very broad, extending up to 510 cm^{-1}), together with a weak peak at 800 cm^{-1} . From our results we can speculate that the first broad feature is consistent with a mixture of W - and Z -carbon, while the second could come from M -carbon. However, these meteorite samples contain a large quantity of impurities and the interpretation of the spectra is delicate. Moreover, another series of sharp peaks in the Raman spectrum is systematically observed at 500 , 1140 , and 1132 cm^{-1} in carbon thin films deposited by chemical vapor deposition, where the sp^2 - sp^3 content varies. Note that the most interesting feature, a narrow vibration at 1150 cm^{-1} , is again consistent with the formation of microdomains of sp^3 carbon structures within the sample (see Fig. 3). These experimental peaks have been up to now interpreted as coming from the formation of “nanocrystalline” diamond.^{49–51}

In summary, in order to distinguish the several sp^3 structures by Raman experiments we propose the use of the following fingerprints: (i) For BcT carbon the most important mode is the B_{1g} mode at 1124 cm^{-1} , that should appear at above 18.0 GPa ; (ii) M -carbon can be identified by the A_g mode at 900 cm^{-1} at around 13.5 GPa ; (iii) for W -carbon the A_g mode is at 1300 cm^{-1} , i.e., below the diamond zone, at more than 12.3 GPa ; and (iv) finally, the transition to Z -carbon at 10 GPa can be identified by the A_g modes at around 1220 and 1090 cm^{-1} . We should emphasize that the calculated frequencies and transition pressures contain an error caused by the theoretical framework. Therefore, a positive and incontestable determination of the structure of compressed graphite will require the identification of several peaks in different frequency ranges. Our results can, however, serve as a useful guide for experimentalists performing this difficult task.

J. A. F. L. acknowledges the CONACyT-Mexico. S. B. acknowledges support from EU’s Seventh Framework Programme (e-I3 Contract No. ETSF). L. L. and M. A. L. M. acknowledge support from the French ANR (Contract No. ANR-08-CEXC8-008-01). Computational resources were provided by IDRIS-GENCI (Project No. x2011096017) in France and the Swiss National Supercomputing Center. Financial support provided by the Swiss National Science Foundation is gratefully acknowledged.

¹F. P. Bundy, *J. Chem. Phys.* **46**, 3437 (1967).

²A. F. Goncharov, I. N. Makarenko, and S. M. Stishov, *Sov. Phys. JETP* **69**, 380 (1989).

³W. Utsumi and T. Yagi, *Science* **252**, (1991)

⁴Y. X. Zhao and I. L. Spain, *Phys. Rev. B* **40**, 993 (1989).

⁵T. Yagi, W. Utsumi, M. A. Yamakata, T. Kikegawa, and O. Shimomura, *Phys. Rev. B* **46**, 6031 (1992).

⁶W. L. Mao, H. Mao, P. J. Eng, T. P. Trainor, M. Newville, C. Kao, D. L. Heinz, J. Shu, Y. Meng, and R. J. Hemley, *Science* **302**, 425 (2003).

- ⁷M. Hanfland, H. Beister, and K. Syassen, *Phys. Rev. B* **39**, 12598 (1989).
- ⁸R. Z. Khaliullin, H. Eshet, T. D. Kühne, J. Behler, and M. Parrinello, *Nat. Mater.* **10**, 693 (2011).
- ⁹A. R. Oganov, *Modern Methods of Crystal Structure Prediction*, 1st ed. (Wiley-VCH, Berlin, 2010).
- ¹⁰A. R. Oganov and C. W. Glass, *J. Chem. Phys.* **124**, 244704 (2006).
- ¹¹C. W. Glass and A. R. Oganov, *Comput. Phys. Commun.* **175**, 713 (2006).
- ¹²R. T. Strong, C. J. Pickard, V. Milman, G. Thimm, and B. Winkler, *Phys. Rev. B* **70**, 045101 (2004).
- ¹³C. J. Pickard and R. J. Needs, *Phys. Rev. Lett.* **97**, 045504 (2006).
- ¹⁴Y. Wang, J. Lv, L. Zhu, and Y. Ma, *Phys. Rev. B* **82**, 094116 (2010).
- ¹⁵S. Goedecker, *J. Chem. Phys.* **120**, 9911 (2004).
- ¹⁶M. Amsler and S. Goedecker, *J. Chem. Phys.* **133**, 224104 (2010).
- ¹⁷Z. S. Zhao, B. Xu, L.-M. Wang, X.-F. Zhou, J. L. He, Z. Y. Liu, H.-T. Wang, and Y. J. Tian, *ACS Nano* **5**, 7226 (2011).
- ¹⁸Q. Zhu, A. R. Oganov, M. A. Salvadó, P. Pertierra, and A. O. Lyakhov, *Phys. Rev. B* **83**, 193410 (2011).
- ¹⁹A. O. Lyakhov and A. R. Oganov, *Phys. Rev. B* **84**, 092103 (2011).
- ²⁰H. Niu, X.-Q. Chen, S. Wang, D. Li, W. L. Mao, and Y. Li, *Phys. Rev. Lett.* **108**, 135501 (2012).
- ²¹R. H. Baugbman and D. S. Galvão, *Chem. Phys. Lett.* **211**, 110 (1993).
- ²²F. J. Ribeiro, P. Tangney, S. G. Louie, and M. L. Cohen, *Phys. Rev. B* **74**, 172101 (2006).
- ²³Q. Li, Y. Ma, A. R. Oganov, H. Wang, H. Wang, Y. Xu, T. Cui, H. K. Mao, and G. Zou, *Phys. Rev. Lett.* **102**, 175506 (2009).
- ²⁴K. Umemoto, R. M. Wentzcovitch, S. Saito, and T. Miyake, *Phys. Rev. Lett.* **104**, 125504 (2010).
- ²⁵X. F. Zhou, G. R. Qian, X. Dong, L. Zhang, Y. Tian, and H. T. Wang, *Phys. Rev. B* **82**, 134126 (2010).
- ²⁶J. T. Wang, C. Chen, and Y. Kawazoe, *Phys. Rev. Lett.* **106**, 075501 (2011).
- ²⁷M. Amsler, J. A. Flores-Livas, L. Lehtovaara, F. Balima, S. A. Ghasemi, D. Machon, S. Pailhes, A. Willand, D. Caliste, S. Botti, A. SanMiguel, S. Goedecker, and M. A. L. Marques, *Phys. Rev. Lett.* **108**, 065501 (2012).
- ²⁸Z. Zhao, B. Xu, X.-F. Zhou, L.-M. Wang, B. Wen, J. He, Z. Liu, H.-T. Wang, and Y. Tian, *Phys. Rev. Lett.* **107**, 215502 (2011).
- ²⁹D. Selli, I. A. Baburin, R. Martoňák, and S. Leoni, *Phys. Rev. B* **84**, 161411(R) (2011).
- ³⁰H. Niu, P. Wei, Y. Sun, X.-Q. Chen, C. Franchini, D. Li, and Y. Li, *Appl. Phys. Lett.* **99**, 031901 (2011).
- ³¹X. Gonze, G.-M. Rignanese, M. Verstraete, J.-M. Beuken, Y. Pouillon, R. Caracas, F. Jollet, M. Torrent, G. Zerah, M. Mikami, Ph. Ghosez, M. Veithen, V. Olevano, L. Reining, R. Godby, G. Onida, D. Hamann, and D. C. Allan, *Kristallogr.* **220**, 558 (2005).
- ³²N. Troullier and J. L. Martins, *Phys. Rev. B* **43**, 1993 (1991).
- ³³J. P. Perdew, K. Burke, and M. Ernzerhof, *Phys. Rev. Lett.* **77**, 3865 (1996).
- ³⁴See Supplemental Material at <http://link.aps.org/supplemental/10.1103/PhysRevB.85.155428> for phonon frequencies calculated with the GGA-PBE functional and tables summarizing pressure coefficients and Grüneisen parameters.
- ³⁵G. Placzek, in *Handbuch der Radiologie* (Akademische Verlagsgesellschaft, Leipzig, 1934), Vol. 6, p. 208.
- ³⁶M. Veithen, X. Gonze, and P. Ghosez, *Phys. Rev. Lett.* **93**, 187401 (2004).
- ³⁷M. Veithen, X. Gonze, and P. Ghosez, *Phys. Rev. B* **71**, 125107 (2005).
- ³⁸S. A. Prosandeev, U. Waghmare, I. Levin, and J. Maslar, *Phys. Rev. B* **71**, 214307 (2005).
- ³⁹F. Occelli, P. Loubeyre, and R. Letoullec, *Nat. Mater.* **2**, 151 (2003).
- ⁴⁰M. Hanfland, K. Syassen, S. Fahy, S. G. Louie, and M. L. Cohen, *Phys. Rev. B* **31**, 6896 (1985).
- ⁴¹H. Boppart, J. van Straaten, and I. F. Silvera, *Phys. Rev. B* **32**, 1423 (1985).
- ⁴²M. I. Eremets, *J. Raman Spectrosc.* **34**, 515 (2003).
- ⁴³M. Popov, *J. Appl. Phys.* **95**, 5509 (2004).
- ⁴⁴Y. Akahama and H. Kawamura, *J. Appl. Phys.* **96**, 3748 (2004).
- ⁴⁵N. Dubrovinskaia, L. Dubrovinsky, R. Caracas, and M. Hanfland, *Appl. Phys. Lett.* **97**, 251903 (2010).
- ⁴⁶B. R. Wu and Ji-an Xu, *Phys. Rev. B* **60**, 2964 (1999).
- ⁴⁷K. Kunc, I. Loa, and K. Syassen, *Phys. Rev. B* **68**, 094107 (2003).
- ⁴⁸D. C. Smith and G. Godard, *Spectrochim. Acta, Part A* **73**, 428 (2009).
- ⁴⁹S. Prawer, K. W. Nugent, D. N. Jamieson, J. Orwa, L. A. Bursill, and J. L. Peng, *J. Chem. Phys. Lett.* **332**, 93 (2000).
- ⁵⁰A. C. Ferrari and J. Robertson, *Phys. Rev. B* **63**, 121405 (2001).
- ⁵¹Sh. Michaelson, A. Stacey, J. Orwa, A. Cimmino, S. Prawer, B. C. Cowie, O. A. Williams, D. M. Gruen, and A. Hoffman, *J. Appl. Phys.* **107**, 093521 (2010).